

# Fragile-to-strong transition and polyamorphism in the energy landscape of liquid silica

Ivan Saika-Voivod,<sup>1</sup> Peter H. Poole,<sup>1</sup> and Francesco Sciortino<sup>2</sup>

<sup>1</sup>*Department of Applied Mathematics, University of Western Ontario, London, Ontario N6A 5B7, Canada*

<sup>2</sup>*Dipartimento di Fisica and Istituto Nazionale per la Fisica della Materia, Universita' di Roma La Sapienza, Piazzale Aldo Moro 2, I-00185, Roma, Italy*

(Dated: October 27, 2018)

We study the static and dynamic properties of liquid silica over a wide range of temperature  $T$  and density  $\rho$  using computer simulations. The results reveal a change in the potential energy landscape as  $T$  decreases that underlies a transition from a fragile liquid at high  $T$  to a strong liquid at low  $T$ . We also show that a specific heat anomaly is associated with this fragile-to-strong transition, and suggest that this anomaly is related to the polyamorphic behaviour of amorphous solid silica.

Liquid silica is the archetypal glass former, and compounds based on silica are ubiquitous as natural and man-made amorphous materials. Liquid silica is also the extreme case of a “strong liquid,” one having a variation of viscosity  $\eta$  with temperature  $T$  that closely follows the Arrhenius law  $\log \eta \sim 1/T$  as the liquid is cooled toward its glass transition temperature  $T_g$  [1, 2]. In contrast, most liquids are to some degree “fragile,” exhibiting significantly faster-than-Arrhenius increases of  $\eta$  as  $T \rightarrow T_g$ . Recent studies focusing on the properties of the potential energy hypersurface (PES)—or “energy landscape”—of the liquid have demonstrated the controlling influence of the PES on transport properties as  $T \rightarrow T_g$  [3, 4, 5, 6, 7]. However, these studies have only addressed fragile liquids, and the origin of strong liquid behaviour in terms of the energy landscape has not yet been resolved. It is this question that we address here.

In a molecular dynamics computer simulation of an equilibrium liquid, the diffusion coefficient  $D$  is readily evaluated from the particle trajectories. Like  $\eta$ ,  $D$  is a characteristic transport property whose deviations from the Arrhenius law serve to classify a liquid as strong or fragile. The theory of Adam and Gibbs (AG) [8] states that  $D$  is related to the configurational entropy,  $S_c$  via,

$$D = D_0 \exp(-A/TS_c), \quad (1)$$

where the parameters  $D_0$  and  $A$  are commonly assumed to be  $T$ -independent.  $S_c$  quantifies the number of distinct configurational states explored by the liquid in equilibrium. These states have been proposed to correspond to the “basins” of the PES sampled by the liquid [9, 10]. A basin is the set of points in phase space representing configurations having the same local minimum. The local minimum configuration is termed an inherent structure (IS), and is identified in simulation by a steepest descent minimization of the potential energy.

Following the IS thermodynamic formalism of Stillinger and Weber [9], the internal energy of the liquid can be expressed as  $E = e_{IS} + E_{harm} + E_{anh}$ , where  $e_{IS}$  is the average IS energy and the last two terms are the average contributions to  $E$  due to thermal excitations about the IS.  $E_{harm}$  is the average harmonic contribution determined from a quadratic approximation to  $E$  around each IS minimum, while  $E_{anh}$  is the remain-

ing, necessarily anharmonic contribution. The harmonic and anharmonic potentials characterize the shape of the basin.

If the shape of the basins does not depend on  $e_{IS}$  (a condition satisfied at constant density  $\rho$  in the present study; see Methods), then  $S_c$  can be calculated along an isochore by integrating the  $T$  dependence of  $e_{IS}$  at constant volume  $V$  [4]:

$$S_c = S_c^0 + \int_{T_0}^T \frac{1}{T'} \left( \frac{\partial e_{IS}}{\partial T'} \right)_V dT', \quad (2)$$

where  $S_c^0$  is the value of  $S_c$  at a reference  $T = T_0$  (see Methods). Eq. 2 highlights that the  $T$  dependence of  $S_c$  arises solely from changes in  $e_{IS}$  [4, 9]. Evaluation of  $S_c$  when the basin shape depends on  $e_{IS}$  is also feasible [6, 11, 12].

For a strong liquid that satisfies Eq. 1, the  $T$  dependence of  $S_c$  must approach a constant to recover Arrhenius behaviour. From Eq. 2, if  $S_c$  is constant, then so must be the variation of  $e_{IS}$  with  $T$ . This behaviour would be qualitatively different from that found in simulations of fragile liquids. For example, recent studies of a binary Lennard-Jones liquid have shown that  $e_{IS} \propto -1/T$ , a dependence that results from a Gaussian distribution of IS energies [5, 6]. When the IS energy distribution is Gaussian, fragility has been shown to depend on the total number of IS states, the width of the Gaussian, and the dependence of the basin shape on  $e_{IS}$  [6, 13]. However, it is not known if the PES of a strong liquid is similarly characterized by a Gaussian distribution of IS energies but with parameters that differ from the fragile liquid case, or if the PES is qualitatively different from that of a fragile liquid.

In addition, some analyses of experimental data for silica suggest that the liquid may be fragile at very high  $T$  [14, 15]. Recent simulations [16] of the BKS [17] model of silica between  $T = 2750$  and 6000 K have also shown that at the onset of slow dynamics, as reflected for example by the presence of two-step relaxation in structural autocorrelation functions, BKS silica is a fragile liquid. At about 3300 K BKS silica transforms to a strong liquid and the  $T$ -dependence of all characteristic relaxation times becomes Arrhenius [16]. The relationship of the

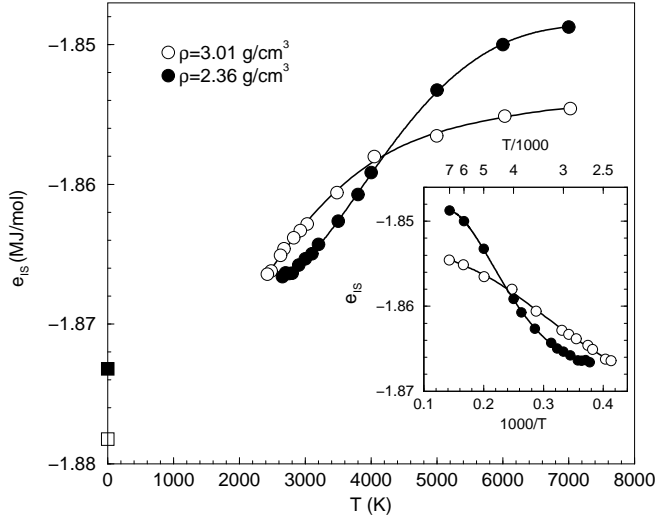


FIG. 1:  $e_{IS}$  as a function of  $T$  along two isochores. At  $T = 0$  we show the energy  $E_0$  of the crystalline system at  $\rho = 2.36 \text{ g/cm}^3$  (filled square) and  $\rho = 3.01 \text{ g/cm}^3$  (open square).  $E_0$  is found by calculating the  $V$  dependence of the potential energy at  $T = 0$  of three crystal polymorphs of silica (stishovite, coesite and quartz), and then using the common tangent construction to determine the potential energy of the heterophase of coexisting crystals that would be the ground state at the required bulk value of  $\rho$ . Inset:  $e_{IS}$  for the same isochores as in the main panel, plotted as a function of  $1/T$ . Only the high density data show a clear  $1/T$  behaviour at low  $T$ .

PES to such a “fragile-to-strong” transition is not yet known.

To address these questions, we conduct extensive equilibrium simulations of BKS silica over a large range of  $T$  and  $\rho$  to examine the fragile-to-strong transition, and to identify the energy landscape behaviour that underlies it. The results clarify our understanding not only of the origins of silica’s status as a strong liquid, but also of the dynamical behaviour of a wider class of liquids that are to some degree silica-like, most notably water and silicon [18], but also other systems such as  $\text{BeF}_2$  [19]. Indeed, the concept of a “fragile-to-strong” transition was first proposed for the case of deeply supercooled water [20].

Fig. 1 shows the  $T$  dependence of  $e_{IS}$  along two isochores. The shape of the higher  $\rho$  isochore is similar to that found for fragile liquids. However, at the lower  $\rho$ —which is close to the experimental  $\rho$  at ambient pressure— $e_{IS}$  exhibits an inflection, passing from concave downward at high  $T$  to concave upward at low  $T$ . Fig. 1 also shows the potential energy  $E_0$  at  $T = 0$  of the corresponding equilibrium crystalline system for the same  $\rho$ . Since the energy of the lowest IS cannot be less than  $E_0$ ,  $E_0$  sets a lower bound on  $e_{IS}$ . The value of  $E_0$  relative to the measured  $e_{IS}$  curves confirms that an inflection occurs.

The inset of Fig. 1 shows that the relation  $e_{IS} \propto -1/T$ ,

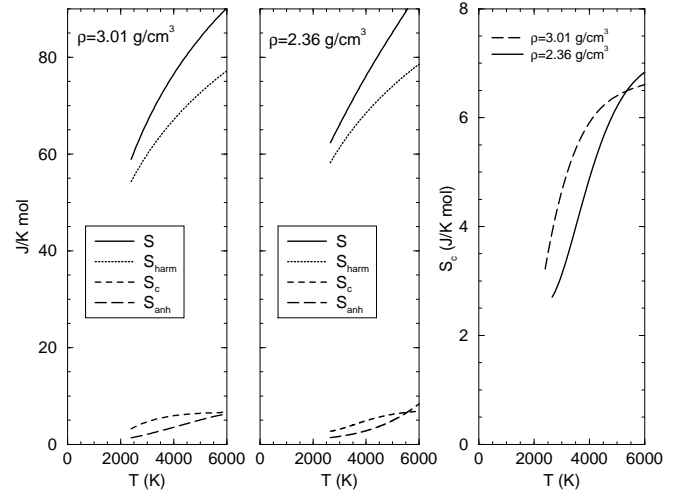


FIG. 2:  $S$  and its component contributions as a function of  $T$  at  $\rho = 3.01 \text{ g/cm}^3$  (left panel) and  $\rho = 2.36 \text{ g/cm}^3$  (centre panel).  $S_c$  as a function of  $T$  along two isochores (right panel).

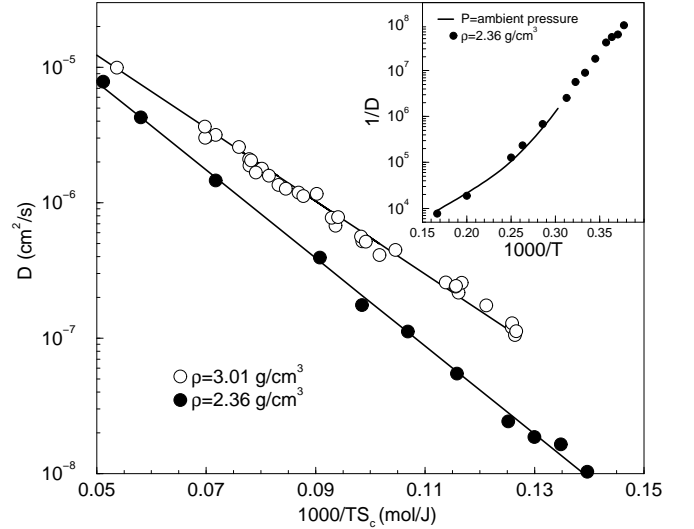


FIG. 3:  $\log D$  versus  $1/T S_c$  along two isochores. Inset: Arrhenius plot of  $1/D$  along the ambient pressure isobar, found by interpolating our isochoric data; and along the  $\rho = 2.36 \text{ g/cm}^3$  isochore. Note the non-Arrhenius to Arrhenius crossover observed both at constant  $\rho$  and at constant  $P$ . All  $D$  values reported here are for Si atoms.

the hallmark of a Gaussian distribution of IS energies, is not obeyed along our lower  $\rho$  isochore. The breakdown of this relation does not arise from changes in the shapes of the basins sampled at different  $T$ . Indeed, the distribution of curvature of the PES around the IS (the vibrational density of states) is found to be independent of the basin depth for all the isochores we study. Hence, within the harmonic approximation, all basins of the same  $\rho$  are characterized by the same vibrational entropy.

Like  $e_{IS}$ ,  $S_c$  (Eq. 2) also exhibits an inflection along our lower  $\rho$  isochore (Fig. 2). In the same range of  $T$ , we find

(Fig. 3) that along each isochore  $D$  satisfies the AG relation within numerical error. That is, despite the change in the nature of the  $T$  dependence of  $S_c$ , the transport properties of the liquid adjust (from non-Arrhenius to Arrhenius) so as to maintain the AG relation, a finding that demonstrates the robustness of Eq. 1 [21, 22]. The low  $\rho$  data thus reveal the signature in the energy landscape of a fragile-to-strong transition. The rapid variation of landscape properties at high  $T$  corresponds to a fragile regime. As  $T$  decreases, the inflections of  $e_{IS}$  and  $S_c$  mark the onset of a regime in which the rate of change of these quantities decreases, consistent with the system's approach to the strong liquid limit.

We note that for the present model,  $S_c$  is much smaller than the vibrational entropy ( $S_{harm} + S_{anh}$ ) and of the same order as  $S_{anh}$ . Moreover, we find that for BKS silica the crystalline vibrational entropy differs significantly from the liquid vibrational entropy, as also found by Richet [2] in his extensive analysis of silicate melts. This confirms that for silica, the identification of the excess entropy (liquid entropy minus crystal entropy) with  $S_c$  may not be adequate [23, 24]. This highlights the value of finding  $S_c$  via the “all-liquid route” [25] implemented here.

The influence of the energy landscape is sufficiently prominent to appear in the total thermodynamic properties [26]. The isochoric specific heat  $C_V$  can be written as  $C_V = C_V^{IS} + 3R + C_V^{anh}$ , where each term is the derivative with respect to  $T$  of the corresponding contribution to  $E$ , and  $R$  is the gas constant. The inflection in the  $T$  dependence of  $e_{IS}$  corresponds to a maximum in  $C_V^{IS}$  (Fig. 4) that is the origin of a  $C_V$  anomaly, in the form of a peak, in the interval of  $T$  corresponding to the fragile-to-strong transition. An analogous  $C_V$  anomaly has recently been predicted to occur in the silica-like liquid  $\text{BeF}_2$  [19], and in theoretical models designed to reproduce a fragile-to-strong transition [27]. High  $T$  experiments that test for this anomaly, though challenging, can thus directly seek the thermodynamic signature of the fragile-to-strong transition in these systems.

The peak we find in  $C_V$  occurs at  $T$  near the temperature of maximum density of BKS silica, and in the vicinity of a maximum of the isothermal compressibility  $K_T$  predicted for this model [28]. Thermodynamic anomalies, such as peaks in  $C_V$  and  $K_T$ , have been associated with the physics of liquid-liquid transitions and with polyamorphism in glasses, i.e. the abrupt pressure-induced transition of a low-density glass to a high-density glass [29]. Polyamorphism is observed experimentally during compression of silica glass, and the  $C_V$  maximum found here may be the thermal anomaly corresponding to polyamorphism's mechanical anomaly. Along different isochores we find that the  $T$  at which the  $C_V$  maximum occurs decreases with increasing  $\rho$ , as would be expected for an anomaly related to polyamorphism in silica.

These observations together suggest that the present fragile-to-strong transition is the dynamical transition corresponding to the thermodynamic crossover in the liq-

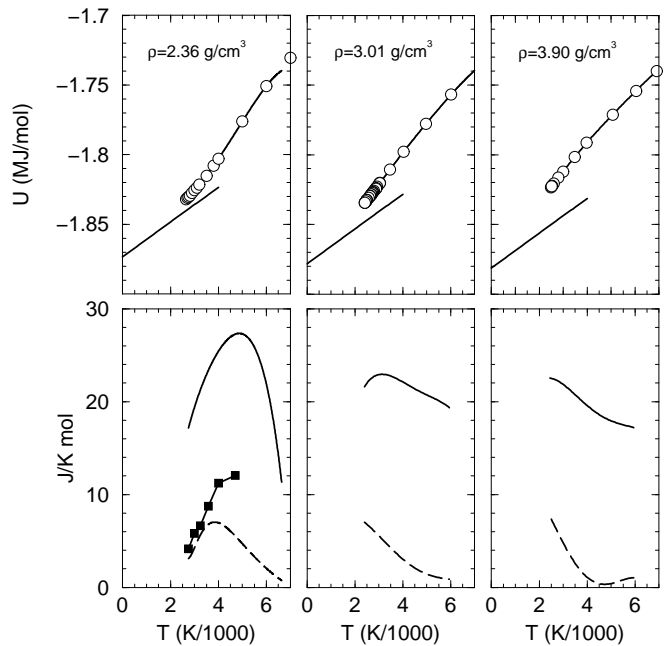


FIG. 4: Upper panels: Isochores of the liquid potential energy  $U$ . Lower panels:  $C_V - (3/2)R$  (solid lines) and  $C_V^{IS}$  (dashed lines) as a function of  $T$ . In the upper panels are shown lines of slope  $\frac{3}{2}R$  whose values at  $T = 0$  are the potential energies of the corresponding crystalline systems, calculated as described in Fig. 1; these lines are lower bounds for  $U$  of the liquid. In the left-most lower panel are shown (filled squares) estimates of the configurational part of  $C_V$  recently evaluated by Scheidler, et al. [31], calculated from the time dependence of the temperature fluctuations.

uid that presages polyamorphism [27]. More generally, our results provide a basis for considering all strong liquids as candidates for polyamorphism: a strong liquid arises via a fragile-to-strong transition, associated with which may be thermodynamic anomalies that are the liquid-state precursors to polyamorphism.

## Appendix: Methods

**Computer simulations:** Results are based on molecular dynamics simulations of BKS silica. All data are obtained from systems of  $N = 1332$  atoms (888 O and 444 Si atoms), except for the  $\rho = 2.36 \text{ g/cm}^3$  isochore, where we employ 999 atoms to facilitate equilibration at low  $T$ . At  $\rho = 2.36 \text{ g/cm}^3$  8 independent runs for each state point are performed. All data reported here are for liquid states in equilibrium. Equilibration is confirmed by ensuring that runs are longer than the slowest relaxation time in the system as evaluated from the collective (coherent) density-density correlation function. The lowest  $T$  runs exceed 80 ns. Simulations are carried out in the constant- $(N, V, E)$  ensemble, and long-range electrostatic interactions are accounted for by Ewald summation. We evaluate  $e_{IS}$  by conducting conjugate gradient minimizations of up to 1000 equilibrium liquid configurations and averaging the results.

*Evaluation of the total entropy:* For a given  $\rho$ ,  $S$  at  $T = T_0 = 4000$  K is calculated using thermodynamic integration: We first find the free energy difference between an ideal gas and a binary mixture Lennard-Jones (LJ) system at the chosen  $\rho$  by integrating the excess pressure along an isotherm from the high  $V$  limit where the system behaves as an ideal gas. We then carry out a set of simulations at constant  $V$  and  $T$  that continuously convert the LJ system to BKS silica, by employing a hybrid potential  $\phi = \lambda\phi_{BKS} + (1 - \lambda)\phi_{LJ}$  [30]. An appropriate thermodynamic integration from  $\lambda = 0$  to 1 yields the free energy of BKS silica, from which  $S$  at  $T_0$  and the chosen  $\rho$  is calculated.  $S$  at other  $T$  is found by further thermodynamic integration at constant  $V$ .

*Evaluation of the vibrational entropy:* We evaluate  $S_{harm}$  from the spectrum of eigenfrequencies  $\nu$  (i.e. the vibrational density of states) calculated from the IS's at each  $T$ , using  $S_{harm} = k \sum_{i=1}^{3N} [1 - \log(h\nu_i/kT)]$ , where  $k$  and  $h$  are Boltzmann's and Planck's constants, respectively. To obtain  $S_{anh}$  we use  $E_{anh}$ . We evaluate  $E_{anh} = E - E_{harm} - e_{IS}$  and then fit  $E_{anh}$  with a polynomial constrained to be zero and have zero slope at  $T = 0$ . When the shape of the basins does not depend on  $e_{IS}$ ,  $S_{anh}$  may be calculated by thermodynamic integration

using the fitted form of  $E_{anh}$  from  $T = 0$  to the desired  $T$ . In terms of the above quantities, the integration constant in Eq. 2 is thus  $S_c^0 = S(T_0) - S_{anh}(T_0) - S_{harm}(T_0)$ .

*Isochoric invariance of basin shape:* Our assumption that the shape of the basins is independent of  $e_{IS}$  along an isochore is based on two observations: (i) We find that the vibrational density of states (the  $\nu$  spectrum) is independent of  $e_{IS}$  along an isochore. (ii) The anharmonic energy of IS configurations heated from  $T = 0$  to a chosen  $T$  follows the  $E_{anh} = E - E_{harm} - e_{IS}$  curve calculated from equilibrium simulations. This is only possible if the anharmonic character of the basins is also independent of  $e_{IS}$ .

### Acknowledgments

We thank C.A. Angell, W. Kob, S. Sastry and R. Speedy for useful discussions. ISV and PHP acknowledge NSERC (Canada) for financial support, and the Compaq-Western Centre for Computational Research for computing resources. FS acknowledges support from the INFM "Iniziativa Calcolo Parallelo," PRE-HOP and from MURST PRIN 2000.

- 
- [1] Angell, C. A. Relaxation in liquids, polymers and plastic crystals - Strong/fragile patterns and problems. *J. Non-Cryst. Solids* **131-133**, 13-31 (1991).
  - [2] Richet, P. Viscosity and configurational entropy of silicate melts. *Geochimica et Cosmochimica Acta* **48**, 471-483 (1984).
  - [3] Sastry, S., Debenedetti, P. G. & Stillinger, F. H. Signatures of distinct dynamical regimes in the energy landscape of a glass-forming liquid. *Nature* **393**, 554-557 (1998).
  - [4] Sciortino, F., Kob, W. & Tartaglia, P. Inherent structure entropy of supercooled liquids. *Phys. Rev. Lett.* **83**, 3214-3217 (1999).
  - [5] Buechner, S. & Heuer, A. The potential energy landscape of a model glass former: thermodynamics, anharmonicities, and finite size effects. *Phys. Rev. E* **60**, 6507-6518 (1999).
  - [6] Sastry, S. The relationship between fragility, configurational entropy and the potential energy landscape of glass-forming liquids. *Nature* **409**, 164-167 (2001).
  - [7] Martinez, L.-M. & Angell, C.A. A thermodynamic connection to the fragility of glass-forming liquids. *Nature* **410**, 663-667 (2001).
  - [8] Adam, G. & Gibbs, J. H. On the temperature dependence of cooperative relaxation properties in glass-forming liquids. *J. Chem. Phys.* **43**, 139-146 (1965).
  - [9] Stillinger, F.H. & Weber, T.A. Packing Structures and Transitions in Liquids and Solids. *Science* **225**, 983-989 (1984).
  - [10] Stillinger, F. H. A topographic view of supercooled liquids and glass formation. *Science* **267**, 1935-1939 (1995).
  - [11] Sciortino, F. & Tartaglia, P. Extension of the Fluctuation-Dissipation theorem to the physical aging of a model glass-forming liquid. *Phys. Rev. Lett.* **86**, 107-111 (2001).
  - [12] Starr, F.W., Sastry, S., La Nave, E., Scala, S., Stanley, H.E. & Sciortino, F. Thermodynamic and structural aspects of the potential energy surface of simulated water. *Phys. Rev. E* **63**, 041201 (2001).
  - [13] Speedy, R.J. Relations between a liquid and its glasses. *J. Phys. Chem. B* **103**, 4060-4065 (1999).
  - [14] Rossler, E., Hess, K.-U. & Novikov, V.N. Universal representation of viscosity in glass forming liquids. *J. Non-Cryst. Solids* **223**, 207-222 (1998).
  - [15] Hess, K.-U., Dingwell, D.B. & Rossler, E. Parametrization of viscosity-temperature relations of aluminosilicate melts *Chemical Geology* **128**, 155-163 (1996).
  - [16] Horbach, J. & Kob, W. Static and dynamic properties of a viscous silica melt. *Phys. Rev. B* **60**, 3169-3181 (1999).
  - [17] Van Beest, B.W.H., Kramer, G.J. & van Santen, R.A. Force fields for silicas and aluminophosphates based on ab initio calculations. *Phys. Rev. Lett.* **64**, 1955-1958 (1990).
  - [18] S. Sastry, private communication.
  - [19] Hemmati, M., Moynihan, C.T. & Angell, C.A. Density Maxima and minima, and water-like heat capacity and transport anomalies, in liquid BeF<sub>2</sub>, *J. Chem. Phys.*, in press (2001).
  - [20] Angell, C.A. Water II is a strong liquid. *J. Phys. Chem.* **97**, 6339-6341 (1993).
  - [21] Speedy, R. J. The hard sphere glass transition. *Mol. Phys.* **95**, 169-178 (1998).
  - [22] Scala, A., Starr, F. W., La Nave, E., Sciortino, F. & Stanley, H. E. Configurational entropy and diffusivity of

- supercooled water. *Nature* **406**, 166-169 (2000).
- [23] Johari, G.P. Contributions to the entropy of a glass and liquid, and the dielectric relaxation time. *J. Chem. Phys.* **112**, 7518-7523 (2000).
  - [24] Goldstein, M. Viscous Liquids and the glass transition: sources of the excess heat capacity. *J. Chem. Phys.* **51**, 3728-3739 (1969).
  - [25] Coluzzi, B., Parisi, G. & Verrocchio, P. Thermodynamical liquid-glass transition in a Lennard-Jones binary mixture. *Phys. Rev. Lett.* **84**, 306-309 (2000).
  - [26] F. H. Stillinger, P. G. Debenedetti and S. Sastry "Resolving Vibrational and Inherent Structural Contributions to Isothermal Compressibility" *J. Chem. Phys.* **109**, 3983, (1998).
  - [27] Jagla, E.A. Fragile-strong transitions and polyamorphism in glass former fluids. preprint, cond-mat/0008218 (2000).
  - [28] Saika-Voivod, I., Sciortino, F. & Poole, P.H. Computer simulation of liquid silica: equation of state and liquid-liquid phase transition. *Phys. Rev. E* **63**, 011202 (2001).
  - [29] Poole, P.H., Grande, T., Angell, C.A. & McMillan, P.F. Polymorphic phase transitions in liquids and glasses. *Science* **275**, 322-323 (1997).
  - [30] Mezei, M. & Beveridge, D.L. Free energy simulations. *Annals of the New York Academy of Sciences* **482**, 1-23 (1986).
  - [31] Scheidler, P., Kob, W., Latz, A., Horbach, J. & Binder, K. Frequency-dependent specific heat of silica. *Phys. Rev. B* **63**, 104294 (2001).